Antarctic Science 24(1), 88–94 (2012) © Antarctic Science Ltd 2011 doi:10.1017/S0954102011000587

Automatic scaling of polar ionograms

CARLO SCOTTO[1,2] and MICHAEL PEZZOPANE[1]*

[1]*Istituto Nazionale di Geofisica e Vulcanologia, Via di Vigna Murata 605, 00143 Rome, Italy*
[2]*Doctoral School in Polar Sciences, University of Siena, Via del Laterino 8, 53100 Siena, Italy*
**corresponding author: michael.pezzopane@ingv.it*

Abstract: The Istituto Nazionale di Geosifica e Vulcanologia (INGV) software for automatic scaling of ionograms (Autoscala) was improved by introducing a system to identify D region absorption events, spread-F condition (frequency spreading in the F region), and Z-ray propagation. The algorithm was applied to a series of ionograms recorded by the AIS-INGV (Advanced Ionospheric Sounder-INGV) ionosonde installed at the Mario Zucchelli Station (74.7°S, 164.1°E), Terra Nova Bay, Antarctica. Critical cases are shown to illustrate the behaviour of the software.

Received 6 April 2011, accepted 2 July 2011, first published online 23 September 2011

Key words: Autoscala, instrument and techniques, ionospheric irregularities, polar ionosphere

Introduction

The polar ionosphere is known to be extremely irregular both spatially and temporally, with a wide range of structures related to complex dynamics and particle precipitation phenomena. Many polar ionograms show that the echo pulse reflected from the F2 layer has a much longer duration (10 times) than the transmitted pulse. This phenomenon is usually referred to as spread-F and many studies have described its morphological and dynamic peculiarities (e.g. Penndorf 1962). Spread-F is caused by scattering from irregularities in the ionosphere across the entire radiation angle of the antenna. In the polar ionosphere such irregularities are field aligned and occur against a background of Travelling Ionospheric Disturbances (TIDs), with horizontal sizes ranging from several tens of meters to about 40 km (Nekrasov *et al*. 1982). Certain types of spread-F are caused by radio aurora, this being the radar signature of the ionization associated with auroral phenomena (Davies 1990).

Another important feature of polar ionograms is the so-called Z-ray, which is a third trace appearing on ionograms, spaced in critical frequency from the ordinary ray (O-ray) by approximately half the electron gyrofrequency. A phenomenon that must be considered when dealing with Z-ray ionograms is resolved frequency spreading. In these cases, ionograms present a duplicate ordinary trace representing reflections from markedly different directions, with the spread in critical frequency indicating a horizontal gradient in the peak electron density (Piggott & Rawer 1972). An ionogram record in which the satellite trace is spaced in critical frequency from the O-ray by half of the electron gyrofrequency, as would be expected of a Z-ray, can lead to an uncertain interpretation of the radio propagation conditions. However, this ambiguity can be resolved by considering that if a satellite trace characterizes the O-ray, a corresponding satellite trace should also characterize the extraordinary ray (X-ray), at least in some part of the record (Bowman 1960).

In the ionograms recorded at the Mario Zucchelli Station (74.7°S, 164.1°E), Terra Nova Bay (TNB), Antarctica, the Z-ray appears as a clean single-line trace only in a minority of cases. At other times this trace is duplicated in the same way as the O- and X-ray traces are duplicated (resolved frequency spreading). In many cases it apparently consists of a number of traces so close that the Z-ray appears diffused. It is also important to bear in mind that the mechanism underlying the reflection of this ray involves the presence of irregularities, which are also responsible for spread-F (Bowman 1960, Papagiannis & Miller 1969).

The problem of an appropriate labelling of ionograms with continuous transitions between the different possible conditions (Z-ray, resolved spread-F, unresolved spread-F) poses a challenge for any automatic scaling software (Reinisch & Huang 1983, Fox & Blundell 1989, Igi *et al*. 1993, Tsai & Berkey 2000, Reinisch *et al*. 2005, Zabotin *et al*. 2006, Ding *et al*. 2007). In this work a possible solution for the automatic detection of these conditions is presented, with the aim of improving the performance of the Autoscala program (Scotto & Pezzopane 2002, Pezzopane & Scotto 2004) in high latitude applications.

Finally, another important phenomenon that is frequently observed at high latitude is the D region absorption event, which can lead to a complete disappearance of any overlying region echo from the ionogram record. This is similar to what occurs at low and mid latitudes during a Sudden Ionospheric Disturbance (SID), when X-rays penetrate to the D region releasing electrons with increasing absorption, resulting in short wave radio blackout. In addition to SIDs, at polar latitudes short wave radio fadeout can be due to Polar Cap Absorption (PCA). These events result from the D region ionizing effect of high-energy protons emitted during solar flares which spiralize around and down the magnetic field lines of the Earth penetrating into the atmosphere near the magnetic poles.

https://doi.org/10.1017/S0954102011000587 Published online by Cambridge University Press

Although a PCA event can last any time from about one hour to several days, while a SID lasts 30–60 min, both phenomena appear on ionosonde records as blank ionograms, indicating absorption effects at lower altitudes due to increased ionization in the D region. These ionograms constitute another challenge for automatic scaling software because they need to be identified and distinguished from cases characterized by spread-F features, and from those in which only the F2 part of the trace is not clearly recorded.

This paper first describes the algorithms added to Autoscala to address the high latitude ionogram features mentioned above, and then some results from the application of this version of Autoscala to a series of ionograms recorded by the AIS-INGV (Advanced Ionospheric Sounder-Istituto Nazionale di Geosifica e Vulcanologia) ionosonde (Zuccheretti *et al*. 2003) installed at TNB.

The method applied by Autoscala

The techniques described in this work to detect D region absorption events, spread-F, and Z-rays are evolutions of the basic algorithm on which Autoscala was originally designed in order to identify the F2 layer (Pezzopane & Scotto 2005, 2007). In this algorithm, the ionogram is initially memorized by Autoscala as a matrix A of m rows and n columns, whose values are defined by the following formulas:

$$m = \text{int}\left[(h'_f - h'_0)/\Delta h'\right] + 1 \qquad (1a)$$

and

$$n = \text{int}\left[(f_f - f_0)/\Delta f\right] + 1\,, \qquad (1b)$$

where $f_f, f_0, \Delta f, h'_f, h'_0$, and $\Delta h'$ are respectively final frequency, initial frequency, frequency step, final virtual height, initial virtual height, and virtual height resolution of the sounding. h'_0 and $\Delta h'$ are fixed values depending upon the design of the ionosonde. For the AIS-INGV h'_0 is 90 km and $\Delta h'$ is 4.5 km. The element a_{ij} (with $i = 1,\ldots, m$ and $j = 1,\ldots, n$) of the matrix A is an integer varying from 0 to 254, this value being proportional to the echo amplitude received by the ionosonde. The automatic scaling procedure starts by defining two empirical curves T_O and T_X that are able to fit the typical shapes of the F2 ordinary and extraordinary traces. The curves are expressed in the following parametric forms:

$$T_O = \begin{cases} f_{ord} = a_{ord} - k \\ h'_{ord} = \text{int}\left\{H_{ord} + A_{ord}\tan\left[\frac{\pi}{2}\cdot\frac{\Delta x - k}{\Delta x}\right]\right\} \\ 0 \le k \le \Delta x \end{cases} \qquad (2a)$$

for the curve used for the investigation of the O-ray, and

$$T_X = \begin{cases} f_{ext} = a_{ext} - k \\ h'_{ext} = \text{int}\left\{H_{ext} + A_{ext}\tan\left[\frac{\pi}{2}\cdot\frac{\Delta x - k}{\Delta x}\right]\right\} \\ 0 \le k \le \Delta x \end{cases} \qquad (2b)$$

for the curve used for the investigation of the X-ray. In Eq. (2a) & (2b) the frequencies and the virtual heights of

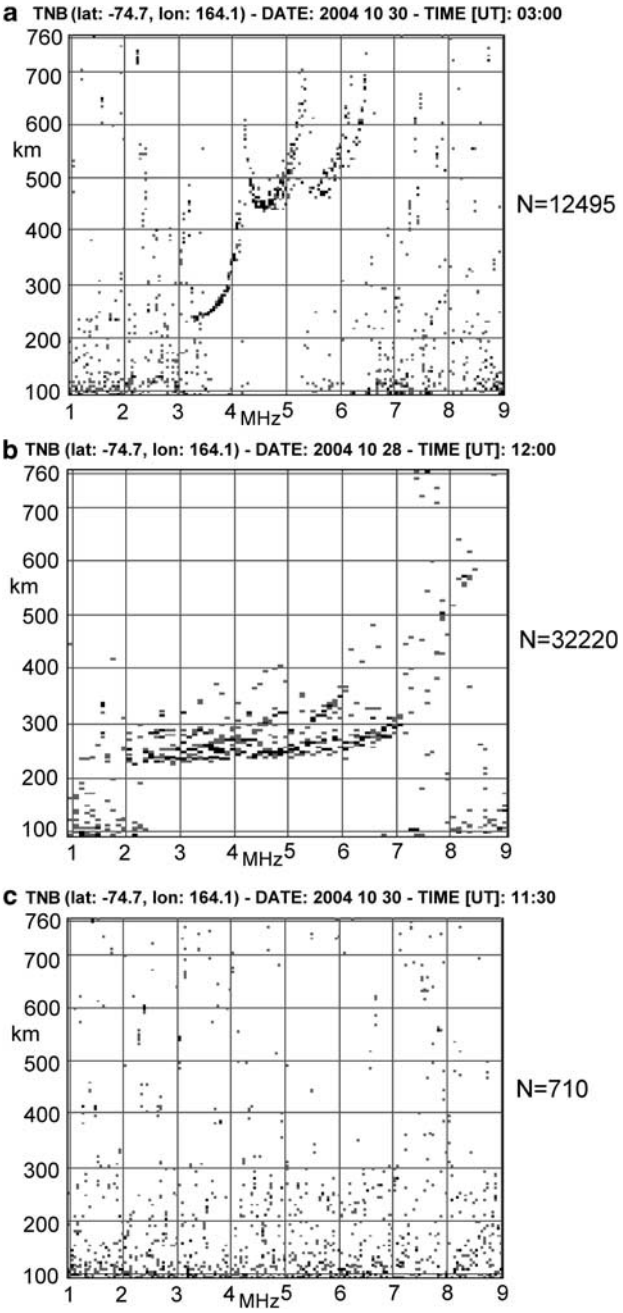


Fig. 1. a. A well-defined ionogram trace, **b.** a spread-F ionogram, and **c.** a blank ionogram, for which the parameter N was equal to 12495, 32220, and 710 respectively. Low N values for blank ionograms is quite a systematic characteristic and was used to intercept these cases, fixing an empirical threshold of $N_t = 3000$.

T_O and T_X are expressed as integers and correspond to the indices i and j of entries a_{ij} of matrix A. The parameters defining the two curves are:

$$H_{ord}, H_{ext}, a_{ord}, a_{ext}, A_{ord}, A_{ext}, \text{and } \Delta x. \qquad (3)$$

H_{ord} and H_{ext} are integers varying from 1 to $(m - 30)$ and correspond to the values of the horizontal asymptote for

https://doi.org/10.1017/S0954102011000587 Published online by Cambridge University Press

T_O and T_X. a_{ord} and a_{ext} are integers varying from 1 to n, with the condition $a_{ord} < a_{ext}$, and correspond to the values of the vertical asymptote for T_O and T_X. A_{ord} and A_{ext}

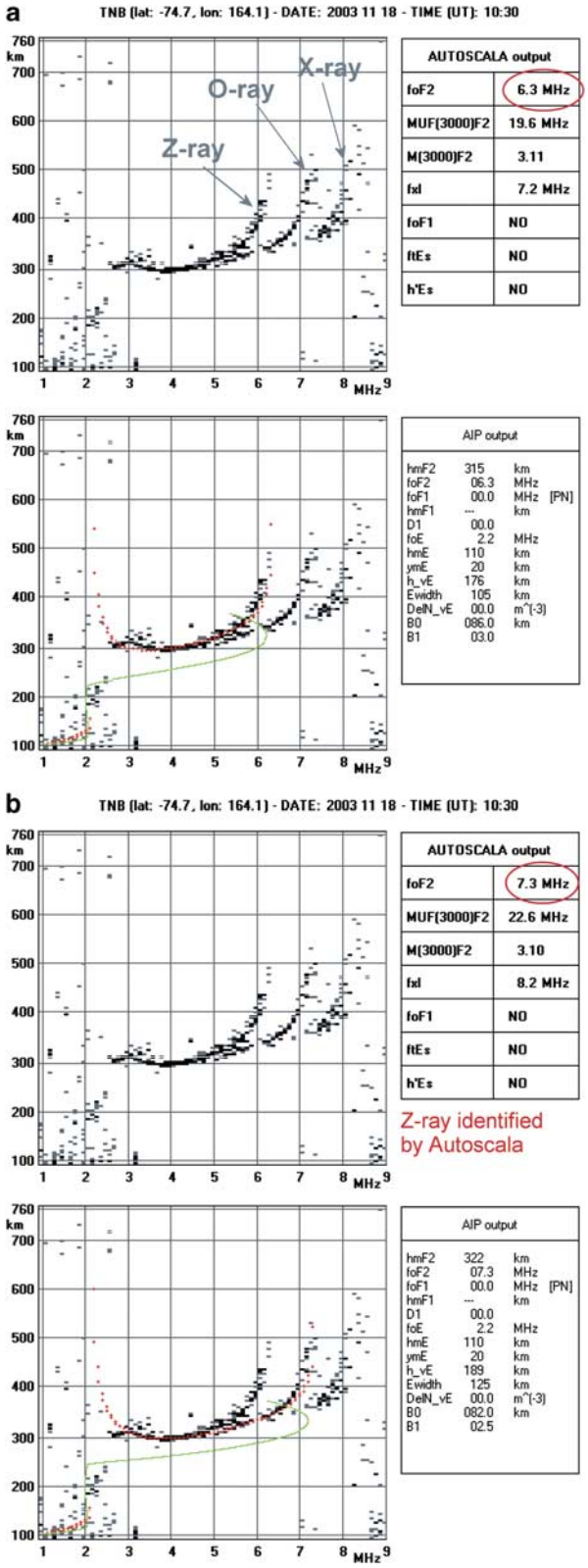


Fig. 2. Ionogram showing triple splitting and the corresponding autoscaling performed by Autoscala **a.** before, and **b.** after defining a third empirical curve T_Z. The top panels contain the original recorded ionogram and the main ionospheric characteristics given as output by Autoscala ("AUTOSCALA output" table). Red ellipses highlight the values of autoscaled *fo*F2 values before and after defining T_Z. Red and green curves in the bottom panels represent the reconstructed O-ray and the corresponding vertical electron density profile, respectively. The "AIP output" table gives the parameters used by Autoscala to estimate the vertical electron density profile associated with the restored ordinary trace.

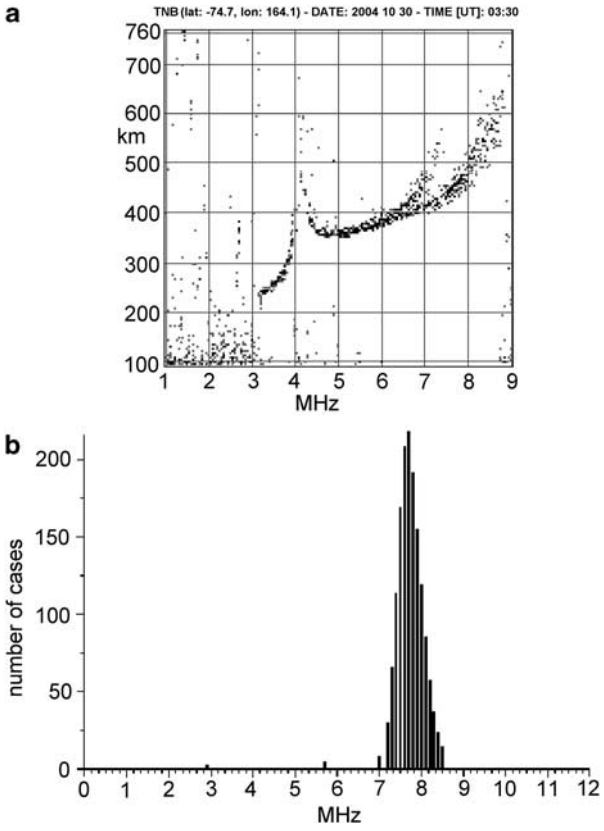


Fig. 3. a. Ionogram for which the F2 trace is well defined, and **b.** the corresponding histogram, showing a well defined single maximum.

are two decimal coefficients. Δx is an integer varying from 6 to 30, representing the frequency interval, expressed in pixels, where T_O and T_X develop. Once Δx is set, the curves start from frequencies (a_{ord} - Δx) and (a_{ext} - Δx) and extend up to a_{ord} and a_{ext} as integer k varies from 0 to Δx. For small values of a_{ord} and a_{ext} it may happen that f_{ord} and f_{ext} are negative, but these values are intercepted and neglected by the algorithm as they correspond to negative values of the frequency.

For each pair of curves T_O and T_X the local correlation $C(H_{ord}, H_{ext}, a_{ord}, a_{ext}, A_{ord}, A_{ext}, \Delta x)$ with the recorded ionogram is calculated and the pair of curves T_O and T_X

https://doi.org/10.1017/S0954102011000587 Published online by Cambridge University Press

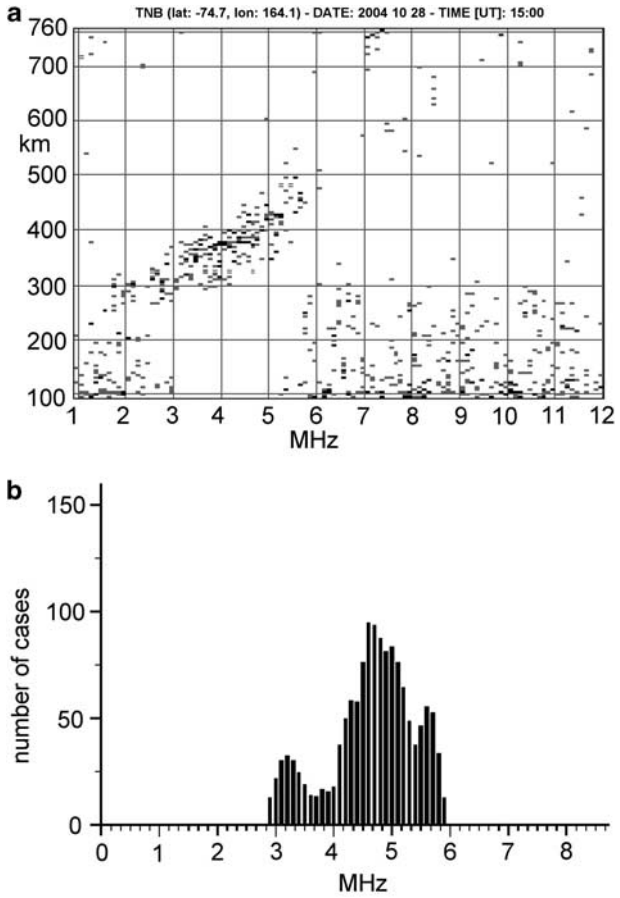


Fig. 4. a. Ionogram for which the F2 trace is not well defined due to the presence of spread-F, and **b.** the corresponding histogram showing multiple maximums.

with the maximum value C_{max} of C are then selected. If C_{max} is greater than a fixed threshold C_t the selected curves are considered as representative of the F2 trace. *fo*F2 is thus obtained as the frequency of the vertical asymptote a_{ord} of T_O, while *MUF*(3000)F2 is numerically calculated by finding the transmission curve tangent to T_O. On the contrary, if C_{max} does not exceed C_t the routine assumes that the F2 trace is not present in the ionogram.

D region absorption event ionogram identification

As noted above, a D region absorption event features as a blank ionogram in ionosonde data, and this absorption is due either to a SID or a PCA. In order to intercept these cases, for each pair of curves T_O and T_X, besides the local correlation C and index I was computed, which makes allowance both for the number of matched points and their amplitude (from 0 to 254). Next, the number N of pairs of curves for which I is greater than a fixed threshold I_t was computed.

Figure 1 shows a well defined trace ionogram, a spread-F ionogram, and a blank ionogram for which N is equal to 12495, 32220, and 710 respectively. A low N value for

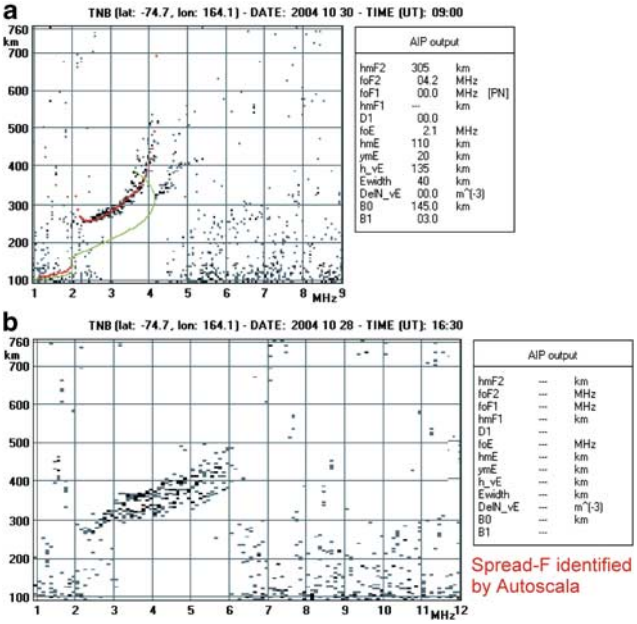


Fig. 5. a. Sufficiently defined ionogram for which Autoscala was able to perform a good scaling providing a reliable estimation of the vertical electron density profile (in red the restored O-ray and in green the corresponding vertical electron density profile). **b.** Spread-F ionogram correctly intercepted by the software and producing no output data. Refer to Fig. 2 for the significance of the "AIP output" table.

blank ionograms is quite a consistent characteristic and can be used to intercept these cases. Therefore, a threshold N_t for N was empirically set, so that cases with $N < N_t$ are interpreted as blank ionograms.

Z-ray identification

In order to identify potential triple splitting (Bowman 1960) characterizing a recorded ionogram trace, in addition to the empirical curves of Eq. (2a) & (2b), the automatic scaling procedure defines a third empirical curve T_Z expressed in the following parametric form:

$$T_Z = \begin{cases} f_z = a_z - k \\ h'_z = \text{int}\left\{H_z + A_z \tan\left[\frac{\pi}{2} \cdot \frac{\Delta x - k}{\Delta x}\right]\right\}. \\ 0 \le k \le \Delta x \end{cases} \quad (4)$$

Three new parameters, H_z, a_z, and A_z, are then defined. H_z is an integer varying from 1 to (m - 30) and corresponds to the value of the horizontal asymptote for T_Z. a_z is an integer varying from 1 to n, with the condition $a_z < a_{ord}$, and corresponds to the value of the vertical asymptote for T_Z. A_z is a decimal coefficient. Once Δx is set, the curve of Eq. (4) starts from the frequency (a_z - Δx) and extends up to a_z as integer k varies from 0 to Δx. For small values of a_z it may happen that f_z is negative, but this value is intercepted and ignored by the algorithm.

https://doi.org/10.1017/S0954102011000587 Published online by Cambridge University Press

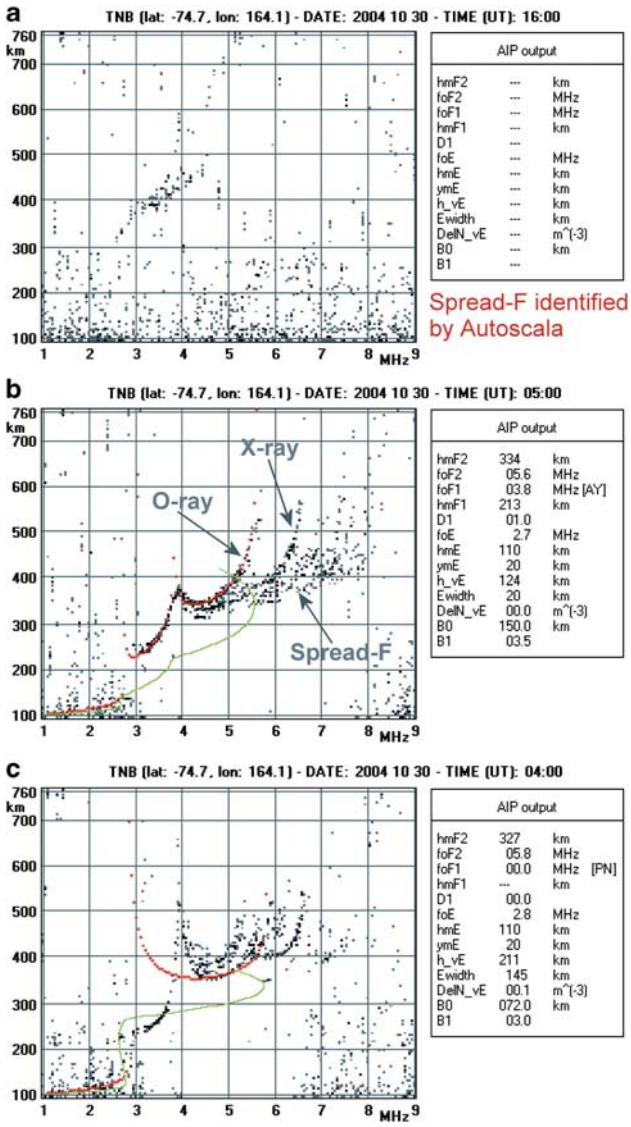


Fig. 6. a. Ionogram in which the action of D region absorption prevents observation of the overlying ionospheric layer echoes except part of the F2 trace. This was automatically scaled as spread-F although a classification as a blank ionogram would have been more appropriate. **b.** Spread-F conditions not impeding a correct scaling of the ionogram which was properly autoscaled. **c.** Spread-F conditions impeding correct scaling of the ionogram which was incorrectly considered as having a well-defined trace, and for which an unrealistic vertical electron density profile was computed. Red and green curves in b. and c. represent the reconstructed O-ray and the corresponding vertical electron density profile, respectively. Refer to Fig. 2 for the significance of the "AIP output" table.

For each tern of curves T_Z, T_O, and T_X, the local correlation $C(H_z, H_{ord}, H_{ext}, a_z, a_{ord}, a_{ext}, A_z, A_{ord}, A_{ext}, \Delta x)$ with the recorded ionogram is calculated making allowance for both the number of matched points and their amplitude, and the tern of curves T_Z, T_O, and T_X with the maximum value C_{max} of C is then selected. If C_{max} is greater than a fixed

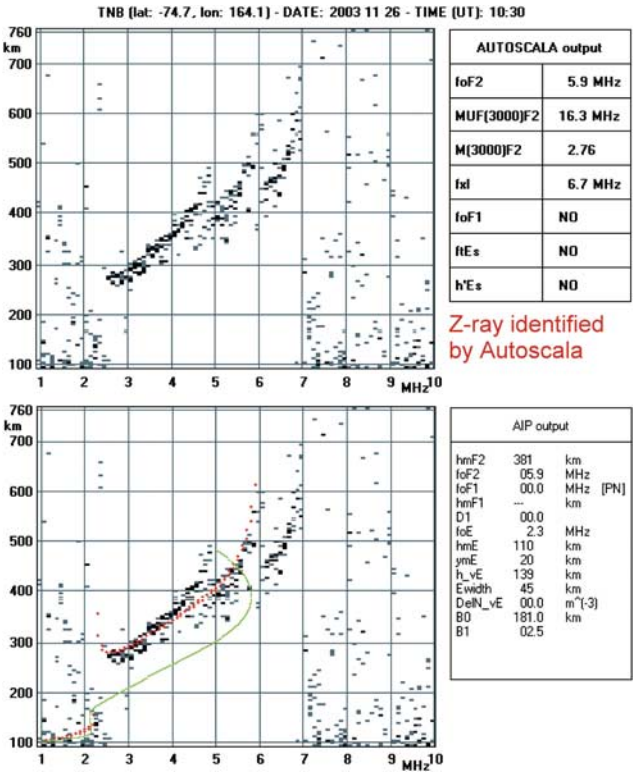


Fig. 7. Ionogram identified by Autoscala as a case of triple splitting but more probably characterized by a spread-F phenomenon. Red and green curves in the bottom panel represent the reconstructed O-ray and the corresponding vertical electron density profile, respectively. Refer to Fig. 2 for the significance of the "AUTOSCALA output" and "AIP output" tables.

threshold C_{tz}, under the condition $C_{tz} > C_t$, the algorithm interprets the presence of triple splitting in the ionogram and the selected curves as representative of the Z-ray, O-ray, and X-ray respectively. On the contrary, if C_{max} does not exceed C_{tz} then the routine assumes that triple splitting is not present.

The introduction of a third curve for identifying potential triple splitting gave quite good results and in this respect Fig. 2 shows the autoscaling performed by Autoscala on an ionogram characterized by a triple splitting before and after defining the third empirical curve T_Z. In Fig. 2 an estimation of the vertical electron density profile (Scotto 2009) is also shown.

Spread-F identification

In order to detect a spread-F condition in ionograms, not only the pair of curves with maximum C value are taken into account, but all curves with a local C correlation exceeding a threshold C_{ts}. All these pairs are considered, retaining the associated parameters in corresponding arrays. Attention is then focused on the parameter a_{ord}, which is associated with the vertical asymptote of T_O. A histogram is defined, reporting the number of curve pairs exceeding C_{ts} as a function of a_{ord}.

https://doi.org/10.1017/S0954102011000587 Published online by Cambridge University Press

Figure 3a shows an ionogram in which the F2 trace is well defined, and Fig. 3b the corresponding histogram. It can be seen that in this case the distribution presents a well defined single maximum. Figure 4a shows an ionogram in which the F2 trace is not well defined due to the presence of spread-F. The corresponding histograms, reported in Fig. 4b, show multiple maximums. This behaviour is quite systematic and can be used as a criterion to differentiate ionograms featuring spread-F from well defined trace ionogram.

Critical cases

Figure 5 shows two examples of the behaviour of Autoscala when applied to non-critical polar ionograms. Figure 5a shows a sufficiently defined trace and Autoscala was able to perform good scaling of the main standard International Union of Radio Science (URSI) parameters, also providing a reliable estimation of the vertical electron density profile. Figure 5b shows an ionogram with a noticeable spread-F and this was correctly intercepted by the software which generated no output data.

By contrast, Fig. 6 shows some examples of the behaviour of Autoscala with some critical ionograms, which exhibit intermediate features and consequently represent a challenge for the software. Figure 6a is an example of an ionogram in which the action of D region absorption is observable, although part of the F2 trace is still present. This trace is not clearly defined but a marked spread-F condition cannot be assumed. In this case the ionogram was automatically scaled as spread-F, although classification as a blank ionogram would have been more appropriate.

Figure 6b & 6c show two different kinds of spread-F ionogram. The second, unlike the first, prevents scaling of the ionogram. While the Fig. 6b ionogram was correctly classified, the Fig. 6c ionogram was incorrectly interpreted as having a well defined trace, producing an unrealistic vertical electron density profile.

As regards Z-ray identification, it can happen that the algorithm interprets a Z-ray to be present when the trace is more probably characterized by a spread-F phenomenon (see Fig. 7), but without doubt this distinction would be very difficult even for an expert operator.

Overall, in a preliminary data analysis performed on 416 ionograms recorded at the Mario Zucchelli Station, there were only 25 definitely wrong cases.

Summary

The high latitude ionosphere is extremely unstable, often characterized by strong D region ionizations, causing absorption events, and by the presence of irregularities that can cause rapid changes in both the amplitude and phase of radio signals passing through them, producing scintillations that seriously degrade trans-ionospheric radio communications. Blank ionograms are the manifestation of absorption events, while Z-ray and spread-F signatures on ionograms are the signs of ionospheric irregularities. An automatic system that was capable of reliably monitoring such features in real time would be very advantageous.

This paper described some new procedures added to Autoscala to address problems with high latitude ionograms. The procedures performed reasonably well, while simultaneously highlighting certain critical cases that can degrade their performance.

Acknowledgements

The constructive comments of the reviewers are gratefully acknowledged.

References

Bowman, G.G. 1960. Triple splitting with the F2-region of the ionosphere at high and mid-latitudes. *Planetary and Space Science*, **2**, 214–222.

Davies, K. 1990. *Ionospheric radio*. London: Peter Peregrinus, 580 pp.

Ding, Z., Ning, B., Wan, W. & Liu, L. 2007. Automatic scaling of F2-layer parameters from ionograms based on the empirical orthogonal function (EOF) analysis of ionospheric electron density. *Earth, Planets and Space*, **59**, 51–58.

Fox, M.W. & Blundell, C. 1989. Automatic scaling of digital ionograms. *Radio Science*, **24**, 747–761.

Igi, S., Nozaki, K., Nagayama, M., Ohtani, A., Kato, H. & Igarashi, K. 1993. Automatic ionogram processing systems in Japan. *In* Wilkinson, P., *ed. Ionosondes and ionosonde networks. Proceedings of the XXIV General Assembly of the International Union of Radio Science, Kyoto, Japan, 25 August–2 September, 1993*. Boulder, CO: WDC-A STP Upper Atmosphere and Geophysics Series, **104**.

Nekrasov, B.Y., Shirochkov, A.V. & Shumilov, I.A. 1982. Investigation of the irregular structure of the polar ionosphere using oblique incidence soundings. *Journal of Atmospheric and Terrestrial Physics*, **44**, 769–772.

Papagiannis, M.D. & Miller, D.L. 1969. Ray-tracing of the Z-mode in a tilted layer ionosphere. *Journal of Atmospheric and Terrestrial Physics*, **31**, 155–165.

Penndorf, R. 1962. Classification of spread-F ionograms. *Journal of Atmospheric and Terrestrial Physics*, **24**, 771–778.

Pezzopane, M. & Scotto, C. 2004. Software for the automatic scaling of critical frequency foF2 and MUF(3000)F2 from ionograms applied at the Ionospheric Observatory of Gibilmanna. *Annals of Geophysics*, **47**, 1783–1790.

Pezzopane, M. & Scotto, C. 2005. The INGV software for the automatic scaling of critical frequency foF2 and MUF(3000)F2 from ionograms: a comparison with the ARTIST system 4.01. *Journal of Atmospheric and Solar Terrestrial Physics*, **67**, 1063–1073.

Pezzopane, M. & Scotto, C. 2007. The automatic scaling of critical frequency foF2 and MUF(3000)F2: a comparison between Autoscala and ARTIST 4.5 on Rome data. *Radio Science*, **42**, 10.1029/2006RS003581.

Piggott, W.R. & Rawer, K. 1972. *URSI handbook of ionogram interpretation and reduction*. Asheville, NC: US Department of Commerce, National Oceanic and Atmospheric Administration, Environmental Data Service, Report UAG 23, 326 pp.

Reinisch, B.W. & Huang, X. 1983. Automatic calculation of electron density profiles from digital ionograms 3. Processing of bottom side ionograms. *Radio Science*, **18**, 477–492.

Reinisch, B.W., Huang, X., Galkin, I.A., Paznukhov, V. & Kozlov, A. 2005. Recent advances in real-time analysis of ionograms and ionospheric drift measurements with digisondes. *Journal of Atmospheric and Solar Terrestrial Physics*, **67**, 1054–1062.

https://doi.org/10.1017/S0954102011000587 Published online by Cambridge University Press

Scotto, C. 2009. Electron density profile calculation technique for Autoscala ionogram analysis. *Advances in Space Research*, **44**, 756–766.

Scotto, C. & Pezzopane, M. 2002. A software for automatic scaling of foF2 and MUF(3000)F2 from ionograms. *Proceedings of the XXVII General Assembly of the International Union of Radio Science, 17–24 August, Maastricht, The Netherlands.* Ghent: International Union of Radio Science, CD-ROM.

Tsai, L.C. & Berkey, F.T. 2000. Ionogram analysis using fuzzy segmentation and connectedness techniques. *Radio Science*, **35**, 1173–1186.

Zabotin, N.A., Wright, J.W. & Zhbankov, G.A. 2006. NeXtYZ: three-dimensional electron density inversion for dynasonde ionograms. *Radio Science*, **41**, 10.1029/2005RS003352.

Zuccheretti, E., Tutone, G., Sciacca, U., Bianchi, C. & Arokiasamy, B.J. 2003. The new AIS-INGV digital ionosonde. *Annals of Geosphysics*, **46**, 647–659.

https://doi.org/10.1017/S0954102011000587 Published online by Cambridge University Press